

## QUADRUPOLE MAGNET DESIGN

Edward A. Taylor

Stanford Linear Accelerator Center, Stanford University, Stanford, California

Summary

A method of computing the quality of field in a quadrupole magnet by means of two-dimensional relaxation is described. The vector potential field at every point in the gap and in the copper is derived, using the given pole tip contour and an irregular pattern of current inputs and assuming infinitely permeable iron. The vector potential is used to calculate flux density at any point in the gap and to estimate flux density in the iron boundaries and in return yokes, and to estimate the inductance of the magnet. The field quality is expressed in terms of its harmonic coefficients, which are directly measurable on the actual magnet. The results of several calculations are presented, which show the effect of changing the location of the windings adjacent to the aperture.

Introduction

In the design of the spectrometers used in the end station of the Stanford Linear Accelerator, several very large and precise quadrupole magnets were required. A numeric method, based on two-dimensional vector potential relaxation was developed, by means of which a programmer of only moderate skill can derive the field of a quadrupole or of any reasonable combination of iron boundaries, air, current inputs or boundaries at infinite distance.

Since the magnets of the Stanford spectrometer are required to work between 5% and full field, the assumption of infinite permeability was considered justified, although, the method of relaxation in the iron using variable permeability is lengthy but straight forward. The corresponding modification of the field in the air is simple, and a good deal faster than the initial relaxation.

The mechanical arrangement used in a typical magnet, our nominal 15" quadrupole, is shown in Figure 1. The clean rectangular form of the parts is expected to minimize the introduction of sub-harmonics in the field, which often are a good deal more serious than the higher harmonics possible in a perfectly symmetrical arrangement.

The contoured portion of the pole tip is being machined on a planer which follows a template to get the correct cross section. A feature not shown on any of the figures, is the shaping of the ends of the pole tip to minimize the change in effective length as the field is increased. The end contours consist of a family of hyperbolas with successively larger pole distances. This portion of the machining is being done by three-dimensional numerically controlled equipment.

Vector Potential vs Scalar Potential

If one assigns a positive potential to one of the poles of a quadrupole, negative to the next one and so on, the sketches in the equipotential lines, it will readily be seen that the principal axes are axes of symmetry and have zero potential. One quadrant is shown in Figure 2(a). The potential field obtained in this way is called a scalar field.

If, on the other hand, as shown in one quadrant in Figure 2(b), the positive and negative potentials are applied to the ends of the current slots and the equipotential lines drawn in, this will represent a vector potential field. These lines evidently correspond to the magnetic lines of force.

The numeric value of each point in either of these fields can be obtained by use of the relaxation rules, and in each case the magnetic flux density at every point is readily obtained.

For a scalar field  $\phi$ ,

$$B_y = \frac{\partial \phi}{\partial y}, \text{ and } B_x = \frac{\partial \phi}{\partial x} \quad (1)$$

for a vector field  $A$

$$B = -\text{Curl } A \quad (2)$$

and since  $A$  is only  $A_z$ ,

$$B_y = \frac{\partial A}{\partial x}, \text{ and } B_x = -\frac{\partial A}{\partial y} \quad (3)$$

Vector fields have one big advantage, and that is the effect of current sources can easily be included in the computation since Poisson's equation obtains:

$$\nabla^2 A = -\mu_0 J \quad (4)$$

where the current term  $\mu_0 J$  can be assigned any arbitrary value if the field is generated entirely by the current sources, which is the only case considered here.

The effect of current sources can be included in the scalar field also, by the use of a modified scalar potential function due to M. H. Blewett, but a degree of skill is required to get valid results.

Scalar potential was the only practical relaxation method until the advent of high speed computers. The reason for this is that the number of passes required to relax a given number of points varies roughly inversely as the number of fixed value points. A comparison of Figure 2(a) with Figure 2(b) will show the advantage of the scalar field in this respect.

An even more serious handicap which the vector potential method has in the speed of relaxation, is the behavior of current points when one is generating a field entirely by its current inputs.

These points literally charge up to their equilibrium potential in the manner of a leaky capacitor being charged with a current source, and all the while the entire field must be "ironed" out.

A final difficulty of the vector potential method is the treatment of iron boundaries. Unlike a scalar iron boundary, which is assigned a fixed value, each point on a vector potential iron boundary has its own potential, which must carry the information on the behavior of the field line at the air-iron interface. The field line may enter at right angles, as in a pole tip of infinite permeability, at a small angle away from perpendicular as for finite permeability, or even run parallel with the iron surface as in the case of a return yoke of infinite permeability.

#### Relaxation Method

The approximations to Laplace's equation which are used for the relaxation of points in a square mesh are well known and are summarized in Figure 3 (a-d). In each case a unit mesh distance is used. Only the cases useful for the vector potential field are given.

Figure 3(e) indicates the method of inserting a current input.  $J$  may have any value since the solution is non-dimensional. For example, a configuration of ours which had about 400 current input points of  $J = .001$  levelled out finally with potentials as high as 6.

#### Boundary Computations

Vector potential requires special treatment at the iron boundaries: this is the most likely step to cause distortions in the derived field due to sloppy arithmetic. The points adjacent to the boundary can be relaxed as in steps 3(c) and 3(d), but then the potential of the boundary points themselves must be adjusted to suit the new values of the adjacent points. If iron of infinite permeability is assumed the field lines must enter the pole tip at right angles to the surface. This is illustrated in Figure 4(a), together with a typical expression for its new potential.

The straight, perpendicular portion of the field line must be as short as possible in order not to distort the field; in general the boundary point assumes the interpolated value of the point where the perpendicular crosses the first mesh line. If the adjacent mesh point is closer than about 0.1 mesh units from the boundary point, the two points will lock together and not relax. In this case the perpendicular must reach a greater distance for its terminal value.

#### Computer Program

The computations described below were written in Fortran II and IV, but the same techniques are applicable in any of the user languages.

Eightfold symmetry can be assumed in a quadrupole, so that only a portion from the  $x$  axis to  $45^\circ$  needs be considered. This could be done with reasonable resolution with a network about 30 x 100 points, but for brevity let us consider an 8 x 20 network.

A corresponding network, termed an "Instruction Matrix", Figure 4(b), is read into memory. By means of a "DO" statement and a "Computed Go TO", the computer makes repeated passes up each line, performing the special instruction called for by the number. For instance:

1. Is the normal operation for the majority of points, Figure 3(a).
2. Is the axis of symmetry operation Figure 3(b).
3. Requires the Vector potential at that point, called "A", to be set to 0, and a return to the bottom of the next line.
4. Is a boundary calculation, such as 3(c) or 3(d) followed by a boundary potential operation such as Figure 4(a) for each boundary point and then a return to next line.
5. Is a similar operation to 2, which describes a field line entering the iron vertically, followed by a return to next line.
6. Requires all such points to be set equal to the maximum value reached by the field, describing the condition existing at an infinitely permeable return yoke.

#### Input Data

Each point 4 requires either one or two boundary points to be described. The boundary information consists of an intercept distance  $a$  or  $b$ , Figure 3(d), a slope of the curve at that point,  $\tan \alpha$ , used in Figure 4(a), and finally the potential of the boundary point which can start at zero but must be revised each pass.

The instruction matrix Figure 4(b) usually has a simple geometric form and can be read into memory with a few statements.

#### Relaxation Speed

A quadrupole field can be solved by setting all of the  $A$  values initially to zero and employing the relations as given. The potential values will increase each pass and eventually level off at the correct values, but the process is far too slow, even with a high speed computer. An array of 90 x 25 points could require 6000 passes and take 30 minutes of 7090 time.

The first time saver is over-relaxation: Consider operation Figure 3(a).

$$\text{Let } R = (B+C+D+E)/4 - A \quad (5)$$

$R$  is the "Residual" in relaxation terminology. The revised value of  $A$  is expressed:

$$A' = A + GR \quad (6)$$

in which  $G$ , the "over-relaxation factor", can have a value between 1 and 2. The relaxation speeds up considerably as  $G$  is increased, and finally becomes unstable near  $G = 2$ . Most automatic computation routines have a method for optimizing  $G$ , but we found a fixed value of  $G = 1.8$  worked well.

The second essential device is to let the initial  $A$  values be set closer to the final value rather than simply setting them all equal

to zero. A new arrangement can be run once with guessed values and the final field read out on cards for future use.

The computation can be run a fixed number of passes, or stopped when the relaxation has reached a satisfactory point.

#### Output

The basic output is the potential at each mesh point, and should be reproduced to seven significant digits. The field between each mesh point, by means of Equ(3), is equal to the normalized difference between the mesh point values. The normalization factor is obtained by requiring the  $B_y$  field on the  $x$  axis at the nominal aperture  $y$  radius to be equal to the design pole tip field.

In this way the field at any point can be calculated, and an estimate made of iron flux densities. The flux density in the return yokes is easily estimated since the largest value of  $A$ , which should be at points 6 in Figure 4(b), is a measure of the total flux crossing the air gap from one pole to another.

Since each value of the vector potential allows one to calculate the amount of flux between that point and zero potential, then the inductance of the cross section follows easily using the relationship:

$$L = \frac{8n\phi}{I} \quad (7)$$

in which  $L$  is the low field DC inductance per meter in henrys,  $n$  is number of turns per pole,  $\phi$  is the flux in webers linking the turns  $n$ , and  $I$  is the calculated excitation current for the required field. This excitation current should include no leakage or reluctance losses, since the inductance is at low field. The constant 8, is for the four poles, of course, and also that the flux  $\phi$  estimated from the vector potential also links another  $n$  turns on the adjacent pole.

To arrive at the correct numerical value for  $\phi$ , one must exercise care. The total amount of flux indicated by the maximum value of  $A$  does not link all turns. Strictly speaking, each current input point should have its  $A$  value summed, and the total divided by the number of points, but the operation can be lumped into four or even two pieces with little change in final value.

The average value of  $A$  for this calculation must be scaled correctly, in a manner described above for calculating flux densities in the return yoke, in order to have  $\phi$  in proper units.

A useful form of the output is to extract the second differences of the  $A$  values, either in the  $x$  direction or the  $y$  direction. These second differences are proportional to the gradient of the field, and provide the quickest way to assess the quality of the field, since an ideal quadrupole has a uniform gradient in the region of interest.

If one adds successive second differences in a straight line, say in the  $x$  direction, and compares it with an equal number of typical second differences around mid aperture, the amount

of deviation of field from ideal can be seen. This has been done on Figure 5; in which the error in the field values  $B_y$  have been plotted against  $x$  for three horizontal rows corresponding to row 1, which is the  $x$  axis, row 6, and row 13. These plots have been done for four different arrangements: the full winding and then for each of the turns  $A$ ,  $B$ , and  $C$ , successively removed. It is apparent that the quality of field is not described adequately by the amount of fall-off of field from ideal along the  $x$  axis, as is customary, or along any other line for that matter. A little change made in winding position, or modification of the contour of the pole tip, improves one area at the expense of another.

#### Harmonic Analysis

It was suggested by C. Peck that for magnet optics purposes, a harmonic analysis of the vector potential would provide the best description of the field and a means of calculating first and second order aberrations in the use of these lenses.

This is a particularly interesting idea, since, as noted above, the  $A$  values are a measure of the total flux between a given point and the zero  $A$  value which exists, for instance, at the center of the aperture. Thus, if one swings an arc about the center, and interpolates for the  $A$  value at each crossing of a mesh line, one obtains a set of values which are proportional to the voltage induced in a coil rotated in a quadrupole field. These values, as a function of their corresponding angular measure, may be reduced to a set of harmonic coefficients in the same way that the harmonic analyzer used by the magnet measurement group measures the quality of a quadrupole field.<sup>1</sup> This analysis was performed by John Levy in a least squares fitting routine.<sup>2</sup>

If a quadrupole has perfect physical symmetry, the vector potential at radius  $a$  may be written:

$$A = A_2 a^2 \cos 2\theta + A_6 a^6 \cos 6\theta + A_{10} a^{10} \cos 10\theta + A_{14} a^{14} \cos 14\theta \quad (8)$$

In the results below, the radius  $a$  in each case is normalized to 1, and the coefficients are given as percentages of  $A_2$ , the quadrupole coefficient.

#### Results

A variety of quadrupole configurations were run, varying such things as coil slot width, radial distance to the conductors, radial width of the conductor bundle and so on. It soon became apparent the factors which control quadrupole field quality are quite inflexible, and all one can do, once the principle parameters of the magnet are fixed, is to play with the windings closest to the aperture, moving them nearer or farther from the center, or leaving out turns.

Thus, Figure 6 summarizes the calculations for three magnets, a 15" quad and two 11" quads, one of which has smaller windings with higher current density because the overall size of the magnet was restricted. In each magnet the

coefficients are given for the full coil and for leaving out one turn at a time, and finally for the middle turn driven in reverse.

### Conclusions

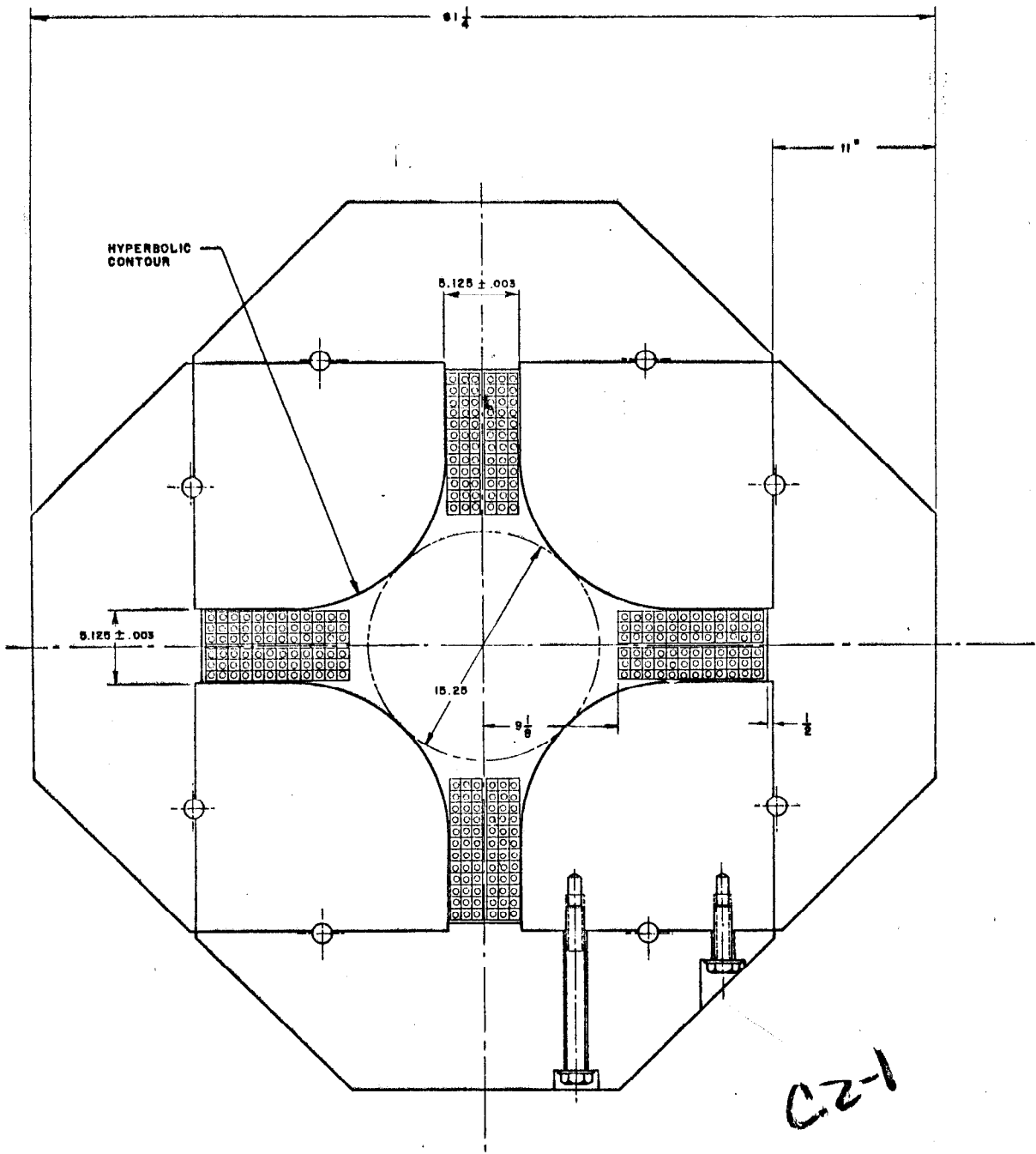
With respect to the configuration of Figure 1, one would be safe in deducing these rather obvious rules for obtaining the best quadrupole field.

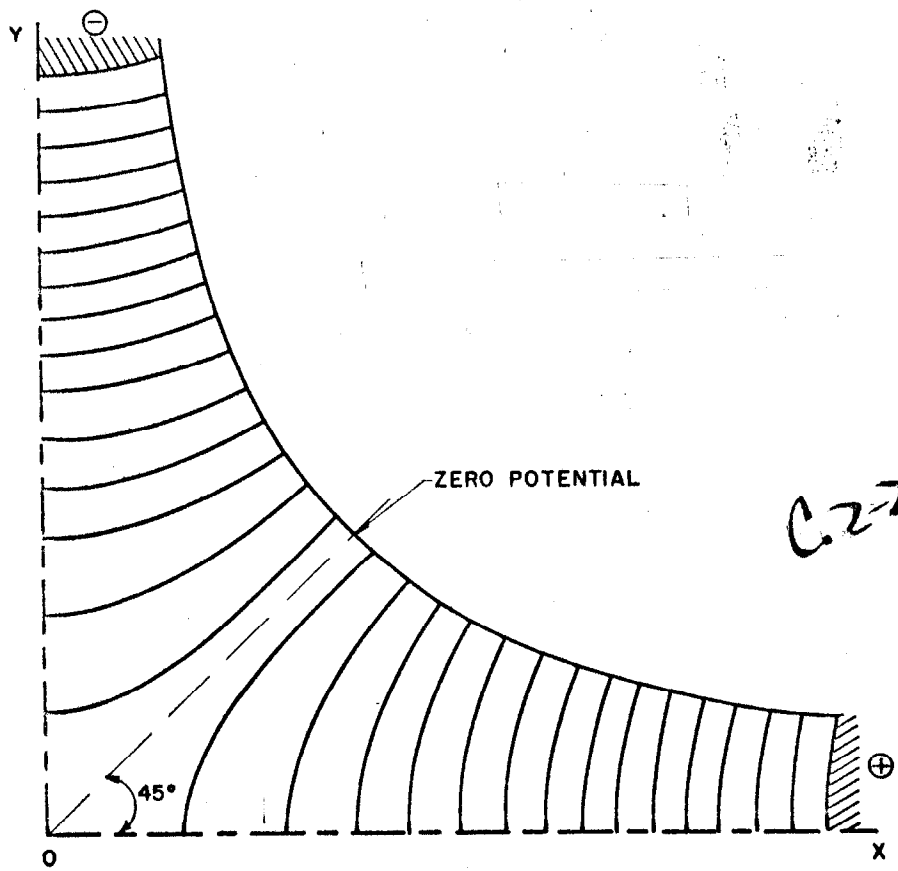
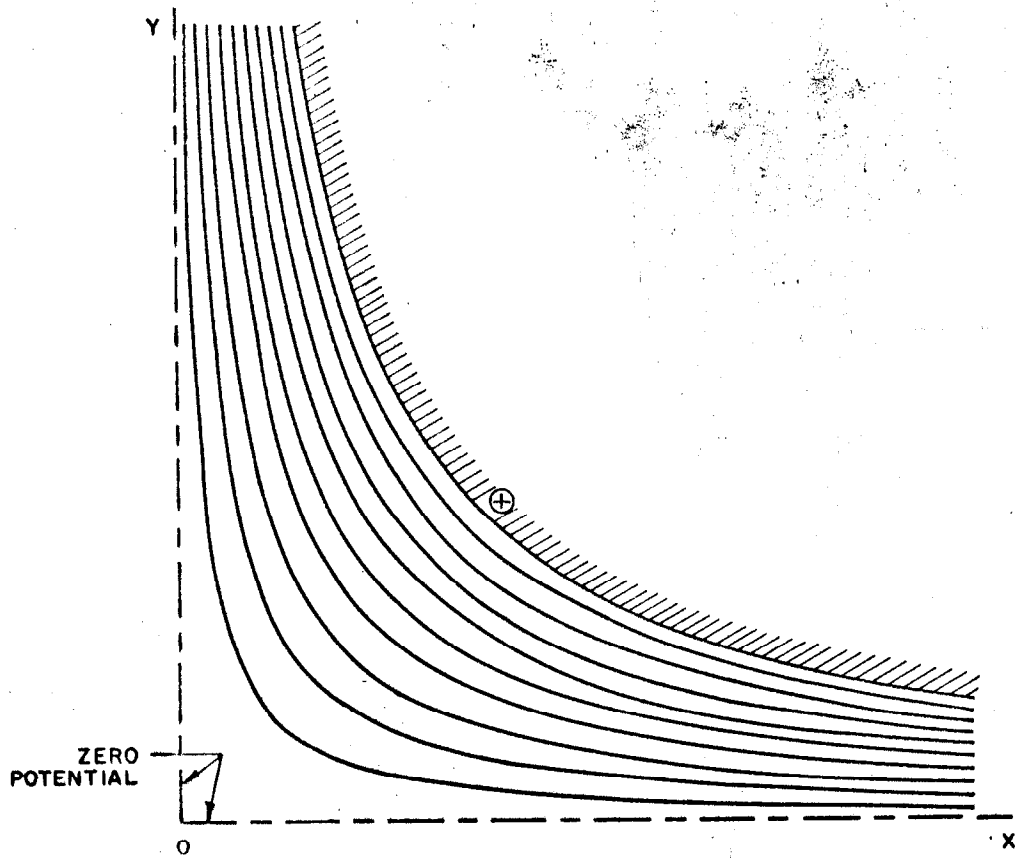
1. Make the mechanical design as simple and rigid as possible, since often the multipoles which are not supposed to exist, can greatly exceed all other errors.
2. Make the pole tip contours simple hyperbolas, as broad as possible. Naturally the longer the contour, the narrower the current slot, permitting only low field magnets, unless very high current density is used.
3. If the current slot is narrow, keep the windings away from the aperture. If you are forced to have a wide current slot, as in our 11" quads, the normal fall off of the field along the principal axis can be compensated by moving the windings closer to the aperture, and in a sense, employing correction windings.
4. The amount of flux which has to go through the return yokes is reduced if high density windings, close to the aperture, are used. This is the choice for quads which must have fields above 13 kilogauss at the pole tip.

---

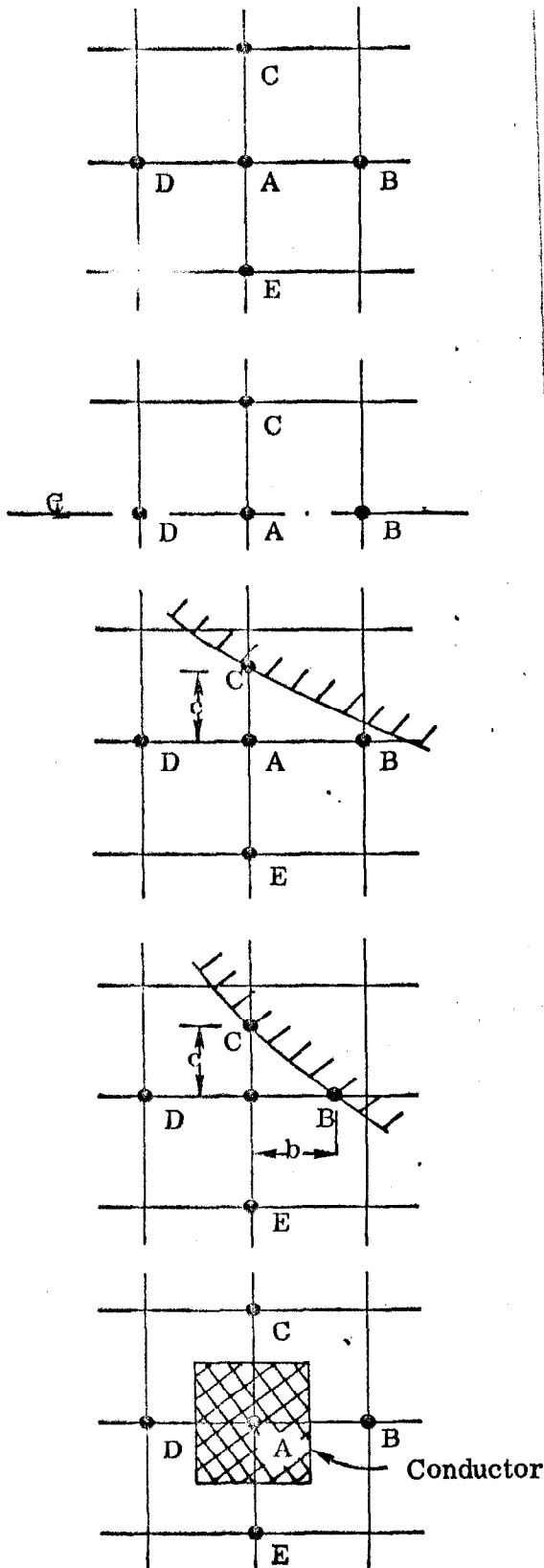
<sup>1</sup>J. K. Cobb and J. J. Murray, "Magnetic Field Measurement and Spectroscopy in Multipole Fields" SLAC Report Number 39.

<sup>2</sup>J. Levy, "Harmonic Analysis of Vector Potential Fields", SLAC TN-65-69.





C.22



(a) For the most general point

$$A = (B + C + D + E)/4$$

(b) For an axis of symmetry in which another point C is implied below A

$$A = (B + 2C + D)/4$$

(c) When the presence of a boundary causes one point to be closer than the normal mesh distance

$$A = (B + C/c + D + E)/(3 + 1/c)$$

(d) When the presence of a boundary causes two points to be closer than the normal mesh distance

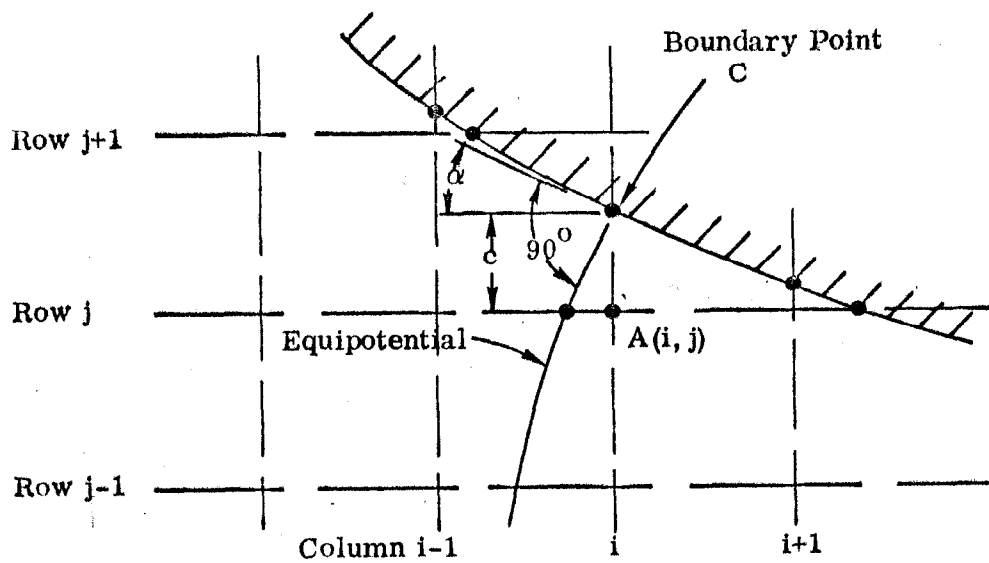
$$A = (B/b + C/c + D + E)/(2 + \frac{1}{b} + \frac{1}{c})$$

C.2-3

(e) For a point at which a current input is desired

$$A = (B + C + D + E)/4 + J$$

Figure 3. Approximations used for relaxation.



$$C = A(i, j) - c \tan \alpha (A(i, j) - A(i-1, j))$$

Figure 4(a). Typical calculation of the potential of an iron boundary point.

C2-4

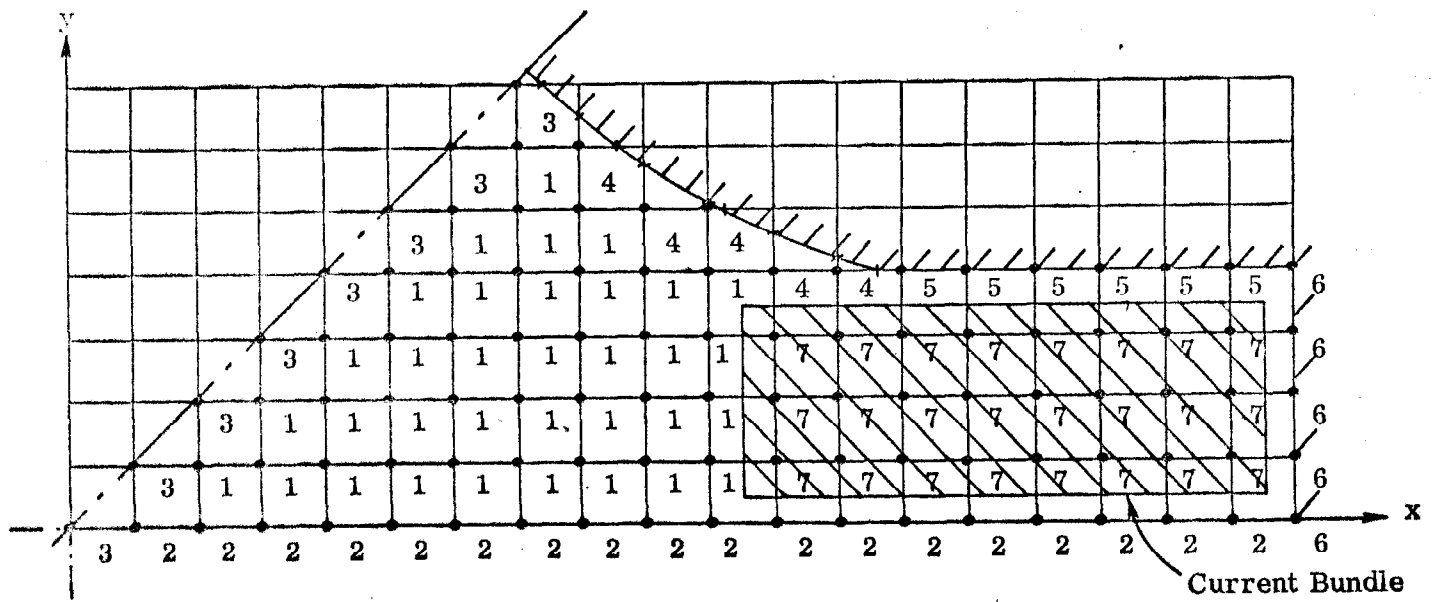
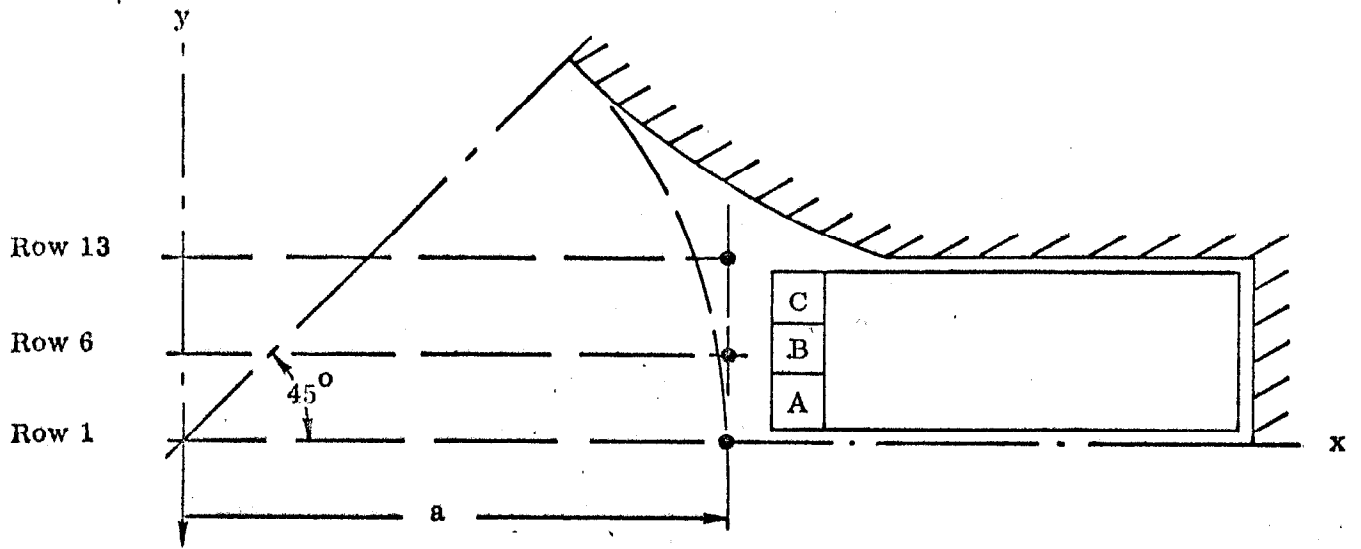


Figure 4(b). Instruction matrix.





C2-5

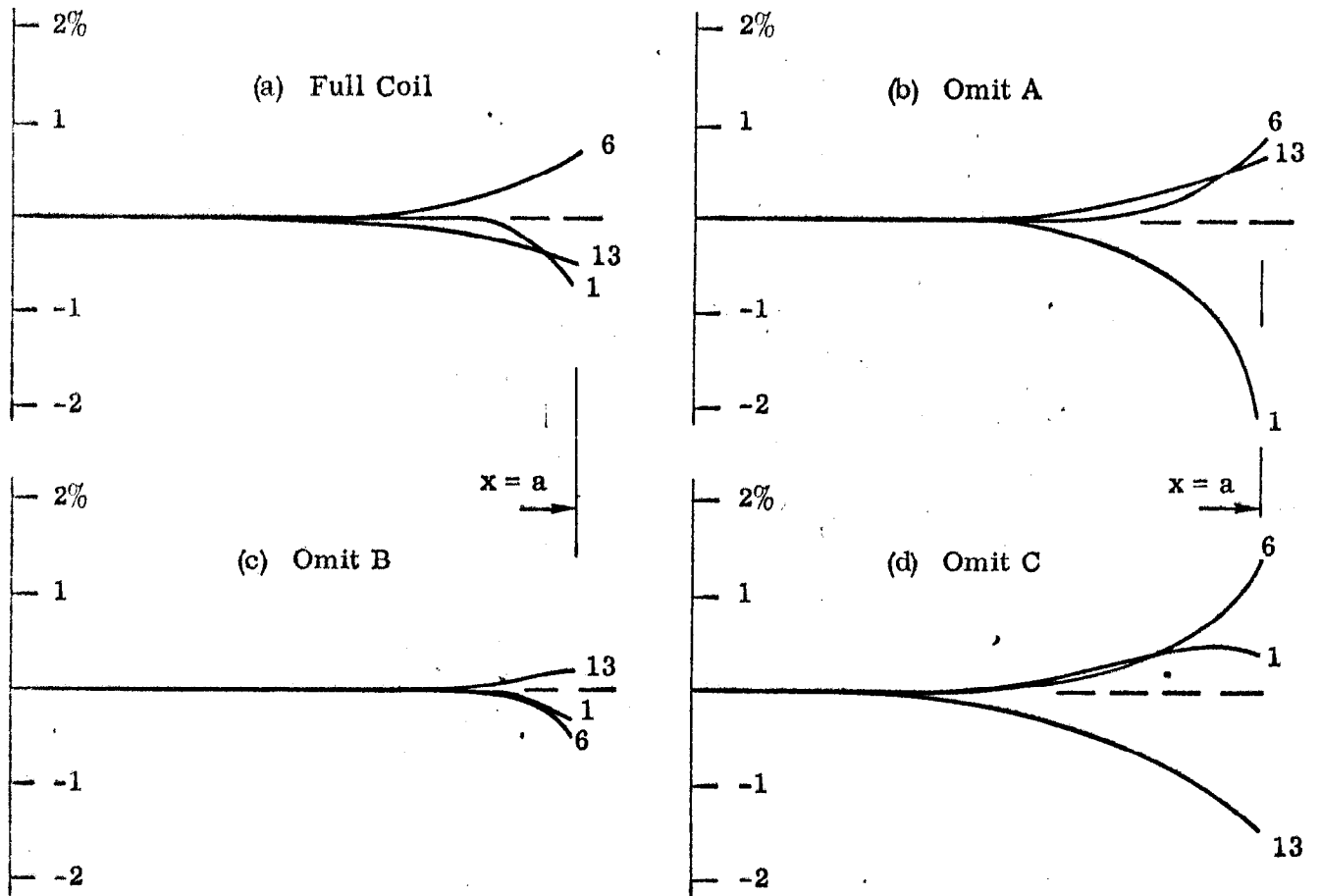
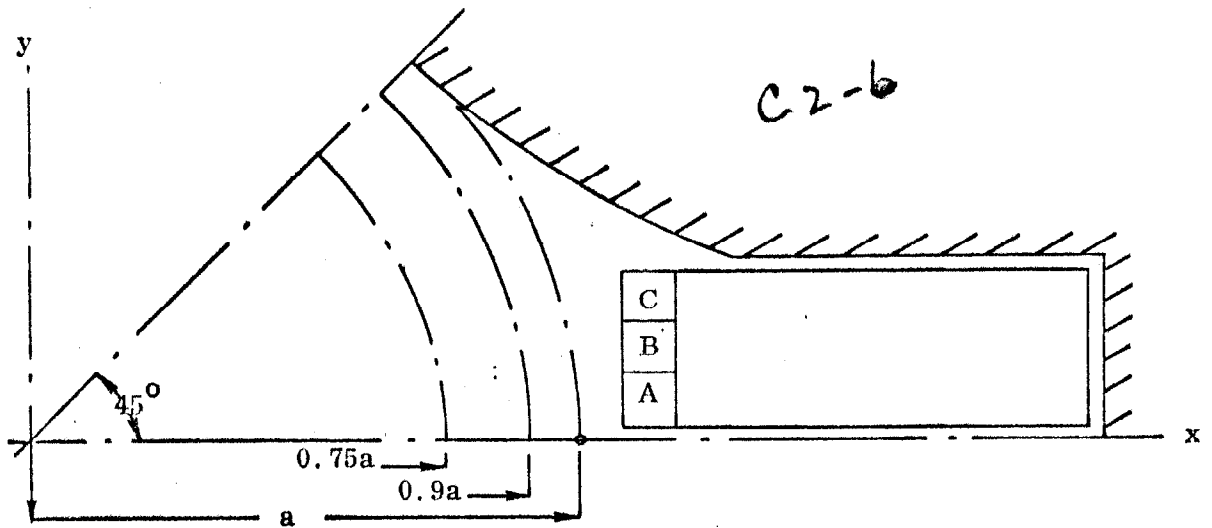


Figure 5. Plot of error  $B_y$  vs.  $x$ .



		Full Winding	Omit A	Omit B	Reverse B	Omit C
<b>15" Quad</b>						
at R = .9a	60/20	.054%	.014	.044	.033	.086
	100/20	.004	-.011	.002	.000	.016
	140/20	-.003	-.006	-.002	-.001	.000
at R = .75a	60/20	.026	.007	.021	.016	.042
	100/20	.001	-.003	.000	.000	.004
	140/20	.000	-.001	.000	.000	.000
<b>11" Quad-High Density Coils</b>						
at R = .9a	60/20	.058	-.066	.014	-.032	.158
	100/20	-.010	-.060	-.015	-.019	.030
	140/20	-.014	-.027	-.006	.002	-.006
at R = .75a	60/20	.028	-.032	.007	-.016	.076
	100/20	-.002	-.014	-.003	-.005	.007
	140/20	-.002	-.003	-.001	.000	-.001
<b>11" Quad-Normal Density Coils</b>						
at R = .9a	60/20	.030	-.051	.001	-.046	.093
	100/20	-.014	-.046	-.016	-.031	.012
	140/20	-.010	-.019	-.006	-.001	-.006
at R = .75a	60/20	.015	-.025	.001	-.014	.045
	100/20	-.003	-.011	-.004	-.005	.003
	140/20	-.001	-.002	-.001	.000	-.001

Figure 6. Harmonic Content of various quadrupoles.